The SLAC High-Density ^{3}He Target Polarized by Spin-Exchange Optical Pumping

H. Middleton[c], G.D. Cates[c], T.E. Chupp[b], B. Driehuys[c], E.W. Hughes[d], J.R. Johnson[e], W. Meyer[d], N.R. Newbury[c], T. Smith[b], and A.K. Thompson[a]

[a] *Department of Physics, Harvard University, Cambridge, MA 02138*
[b] *Randall Laboratory of Physics, University of Michigan, Ann Arbor, MI 48109*
[c] *Joseph Henry Laboratories of Physics, Princeton University, Princeton, NJ 08544*
[d] *Stanford Linear Accelerator Center, Menlo Park, CA 94025*
[e] *Department of Physics, University of Wisconsin, Madison, WI 53706*

Presented by H. Middleton

ABSTRACT

A new high-density ^{3}He target polarized by spin exchange with optically pumped rubidium vapor has recently been used at the Stanford Linear Accelerator in an experiment to measure the longitudinal spin-dependent structure function of the neutron. The ^{3}He target operated at a density of 2.3×10^{20} atoms/cm^3 in a 30 cm long scattering region with polarizations between 30% and 40% measured with NMR techniques. Target cells with several day spin-relaxation times were developed in order to achieve these polarizations.

INTRODUCTION

Polarized ^{3}He has long been recognized as an important nuclear target [1] for studying, among other things, spin-dependent neutron interactions [2,3]. This particular polarized ^{3}He target was constructed for use in experiment E142 at SLAC, a measurement of neutron spin-dependent structure functions [4] which involves measuring an asymmetry in the deep inelastic scattering of polarized electrons from polarized ^{3}He.

The Pauli exclusion principle provides a conceptual understanding of why polarized ^{3}He may be thought of as a polarized neutron, so far as the spin is concerned. Since the two protons spend most of their time in a spatially symmetric S state, their spins must be anti-aligned to satisfy the Pauli principle. Woloshyn has made detailed calculations of the ^{3}He nuclear wavefunction and found that the neutrons in a 100% polarized ^{3}He sample have an 87% polarization while the protons have only a 2.7% polarization, leaving the neutron spin as the dominant contribution to spin dependent scattering [2].

A more traditional approach is to use polarized deuterium as a polarized neutron target [5,6]. The deuterium nuclear wavefunction is better understood than that of ^{3}He, which reduces related systematic errors. The deuteron spin, however, is the result of about equal contributions from neutron and proton spins. Thus, the resulting understanding of the neutron is limited by one's understanding of the proton.

POLARIZING ^{3}He

There are two primary methods of polarizing ^{3}He nuclei for target applications, the metastability exchange procedure first demonstrated by Colegrove, Schearer, and Walters [1] and the method of collisional spin exchange with optically pumped alkali-metal vapor introduced by Bouchiat, Carver, and Varnum for the case of ^{3}He [7], and developed more generally by Happer [8,9]. Both methods have been developed for use in targets by a number of groups [10–16].

The metastability exchange process involves direct optical pumping of the 1.08μm line in ^{3}He. The net spin-exchange rates to the nucleus are reasonably high and the build-up of polarization occurs with time constants of a few seconds. These spin-exchange rates lead to high polarizations of 50% to 70% and make this an excellent system for internal targets in storage rings. The one drawback of this method is the need to produce the metastable ^{3}He atoms in an RF discharge at pressures of a few Torr. This constraint has so far limited metastability exchange targets to a few $\times 10^{19}$ atoms/cm^3 in fixed targets, although cryogenic and mechanical compression techniques are continually improving the ^{3}He density [14,17].

In contrast to metastability exchange, collisional spin exchange with optically pumped alkali-metal vapors can take place at high pressures without sacrificing polarization, but with much slower spin-exchange rates. Spin-exchange optical pumping is a two stage process which begins with optical depopulation pumping of an alkali-metal vapor, in our case, rubidium. The optical pumping is accomplished by illuminating Rb vapor with circularly polarized laser light tuned to the Rb D_1 line, which is the transition from the $5S_{1/2}$ ground state to the $5P_{1/2}$ first excited state. The result is a spin polarization of the valence electron. Under typical optical pumping conditions with optically thick Rb vapors, the Rb is nearly 100% polarized since the photon–rubidium spin-exchange rate is $\sim 10^{-6}$s compared to a depolarizing spin-destruction rate of $\sim 10^{-3}$s [18,11,12]. In principle any alkali-metal vapor can be polarized in this manner, but Rb is particularly convenient due to the commercial availability of Ti:Sapphire lasers, which provide several Watts of cw light and are easily tunable to the 795 nm Rb D_1 resonance.

Once the Rb vapor is polarized, that polarization is transferred to the ^{3}He through spin-exchange collisions [7,19,9]. During any Rb–^{3}He binary collision there is a small probability that the wavefunction of the Rb valence electron will penetrate through the ^{3}He atom's electron cloud to the ^{3}He nucleus. The hyperfine interaction between the ^{3}He nucleus and the Rb valence electron can then induce both species to flip their spins, thereby transferring angular momentum to the ^{3}He nucleus from the electron. The cross section for this interaction is very small, $\sim 10^{-24}$cm^2 [19]. Consequently, the spin-exchange process is very slow. In targets, typical time constants for the build-up of a ^{3}He nuclear polarization are 4 to 40 hours, even though the ^{3}He is in constant contact with the $\approx$ 100% polarized Rb vapor.

TARGET OVERVIEW

Any spin-exchange optically-pumped polarized ^{3}He target will have as its central feature the containment vessel for the Rb and ^{3}He. In our case this is a 170 cm^3 glass cell containing $\approx$ 8.4 atm of ^{3}He at 20°C and $\approx$ 65 Torr of nitrogen, which serves to increase the efficiency of the optical pumping. The target cell has a double chamber design [12], with the two cylindrical chambers having roughly the same volume and connected by a narrow transfer tube. The lower chamber is the target chamber through which the electron beam passes and has a 30 cm long interaction region. The upper chamber, or pumping chamber, is where the optical pumping occurs and contains a few mg of Rb metal.

The layout of the target system is shown in Fig.1. At the center is the target cell. An oven which encloses the pumping chamber of the cell is used to control the Rb vapor density for optical pumping. The Rb density [Rb] is a few times 10^{14} atoms/cm^3 in the pumping chamber (160 to 165 °C) and three orders of magnitude less in the colder, $\approx$65 °C, target chamber. At these temperatures, the pressure in the cell is 11 atm. which corresponds to a ^{3}He number density in the target chamber of 2.3×10^{20} nuclei/cm^3 or a target thickness of 7×10^{21} nuclei/cm^2.

Five Ti:Sapphire lasers provide the photons for the optical pumping. Each Ti:Sapphire is pumped by a 20 W argon ion laser. This system can routinely produce 20 W at the Rb D_1 resonance. The beams pass through focusing/expanding optics and then a quarter-wave plate before being introduced into the pumping chamber of the cell. The five beams enter the chamber through the same window and are arranged to get maximum filling of the chamber's cross section.

A set of 1.4 m Helmholtz coils provides a 20–40 G alignment field for the ^{3}He nuclear po-

larization. This field strength is sufficient to suppress ambient magnetic field inhomogeneities but is still reasonably easy to produce. The ^{3}He nuclear polarization is measured with an Adiabatic Fast Passage Nuclear Magnetic Resonance system [20]. This AFP-NMR system uses, in addition to the main field coils, a set of 18 inch Helmholtz RF drive coils and an orthogonal set of smaller pick-up coils located around the target chamber of the cell. A stronger alignment field would lead to larger NMR signals, but this field strength is an acceptable compromise between signal size and equipment costs.

Finally, all of the target equipment except the lasers and the main Helmholtz coils are located inside a vacuum chamber at a few mTorr pressure in order to reduce the background event rates from non-target materials.

TARGET CELL DESIGN CONSTRAINTS

The primary benefit of using the spin-exchange optical pumping method is the ability of the process to work at high target densities. Ultimately, the target thickness is limited by the use of construction materials which are compatible with high polarizations, in particular, aluminosilicate glass. Tests of our glass cell design indicated a pressure limit of 13 to 15 atmospheres. The cells used during the experiment typically operated at ≈ 11 atm.

The glass windows of the target chamber where the electron beam enters and exits the target cell are within the acceptance of the spectrometers, and therefore must be made as thin as possible in order to minimize background events. The pressure tests mentioned previously were performed on cells with 1 cm radius convex windows, $100 - 130\,\mu$m thick over at least 2 mm diameter central region and the cells used in the experiment were also in this range. The background from these windows amounted to 64% of the total events recorded. Hersman has since reported studies on a concave window design where he found a dramatic improvement in strength over the convex design, allowing much thinner windows [21]. In addition to the windows, another 2.8% of the events are from scattering off of the nitrogen in the cell.

Much of the target development effort was directed toward producing high polarizations in the relatively large volume (170 cm^3) target cells. Previous work from our group has produced up to 65% polarizations in 8 cm^3 spherical cells at 9 atmospheres [10], and work at TRIUMF produced successful 38 cm^3 cells [13]. For the SLAC target, these results needed to be achieved in target cells with much larger volumes, more irregular geometries, and larger surface area to volume ratios.

OPTIMIZING ^{3}He NUCLEAR POLARIZATION

The expected ^{3}He polarization, calculated from a simple analysis of spin-exchange and ^{3}He nuclear relaxation rates, starting from $P_{^3\mathrm{He}} = 0$ at $t = 0$, is

$$P_{^3\mathrm{He}}(t) = \left(\frac{\gamma_{\mathrm{SE}}}{\gamma_{\mathrm{SE}} + \Gamma_{\mathrm{R}}}\right) \langle P_{\mathrm{Rb}} \rangle \left(1 - \mathrm{e}^{-(\gamma_{\mathrm{SE}} + \Gamma_{\mathrm{R}})\,t}\right) \tag{1}$$

where γ_{SE} is the spin-exchange rate per ^{3}He atom between the Rb and ^{3}He, Γ_{R} is the relaxation rate of the ^{3}He nuclear polarization through all channels other than spin exchange with Rb, and $\langle P_{\mathrm{Rb}} \rangle$ is the average polarization of the Rb. Maximizing the ^{3}He polarization therefore requires making t very long, maximizing $\langle P_{\mathrm{Rb}} \rangle$ and γ_{SE}, and minimizing Γ_{R}.

The presence of ionizing radiation such as the electron beam is depolarizing to Rb, and therefore can interfere with optical pumping. Furthermore, the radiation tends to darken the glass, reducing laser transmission into the cell. For these reasons, a double chamber cell design was used which allows continuous optical pumping in a chamber spatially separated from the electron beam. The two chambers are connected by a transfer tube, where diffusion times between the chambers are short (tens of minutes) compared to characteristic polarization build-up times, $(\gamma_{\mathrm{SE}} + \Gamma_{\mathrm{R}})^{-1}$. An alternative solution is to use a single chamber cell which is

polarized prior to insertion into the electron beam, and then to allow the polarization to decay while taking data [10].

Since $P_{\rm Rb}$ is $\approx$ 100% wherever the laser light penetrates, $\langle P_{\rm Rb}\rangle$ is maximized by carefully matching the spatial profile of the laser beam to the geometry of the pumping chamber and by adjusting the [Rb] in the chamber so that the absorption length is nearly equal to the length of the chamber. The spin exchange rate $\gamma_{\rm SE}$ is also sensitive to [Rb], and is defined by

$$\gamma_{SE} \equiv \langle \sigma_{\rm SE}\, v\rangle\, [\rm Rb] \tag{2}$$

where, $\langle \sigma_{\rm SE}\, v\rangle = 1.2 \times 10^{-19}$ cm^3/sec is the velocity-averaged spin-exchange cross section for Rb–^{3}He collisions [22,11] and [Rb] should be averaged over the cell. In contrast, the volume of rubidium vapor which can be fully polarized with a given laser intensity will eventually drop off as [Rb] is increased, so $\gamma_{\rm SE}$ cannot be arbitrarily increased without eventually sacrificing $\langle P_{\rm Rb}\rangle$. The optimum Rb density is most easily found by experimentally tuning the pumping chamber temperature to find the highest ^{3}He polarization. The target typically operated with $1/\gamma_{\rm SE} \approx 35-40$ hours. This is a factor of two larger than for a single chamber cell at the same temperature where all the volume, not just half, is being optically pumped. The factor of two loss in spin-exchange rate is not very important in cases where γ_{SE} is somewhat larger than Γ_R.

^{3}He NUCLEAR SPIN RELAXATION

One unavoidable limit to the ^{3}He relaxation time constant, $\tau_{\rm R} \equiv 1/\Gamma_R$ is a ^{3}He–^{3}He dipolar interaction which occurs during binary collisions in the bulk gas [10]. This interaction couples the ^{3}He nuclear spin to the orbital angular momentum of the two ^{3}He atoms and will therefore cause depolarization. The relaxation rate Γ_{bulk} is proportional to the ^{3}He density and varies slightly with temperature, implying a maximum relaxation time constant of 100 hours at the densities and temperatures in the target cells used. This limiting lifetime will be further reduced by relaxation due to collisions with paramagnetic gaseous impurities and cell wall interactions to yield an inherent cell lifetime of

$$\frac{1}{\tau_{cell}} = \frac{1}{\tau_{bulk}} + \frac{1}{\tau_{wall}} + \frac{1}{\tau_{gas}} \tag{3}$$

In addition, there are interactions not inherent to the target cell which further increase the nuclear relaxation rate. Inhomogeneities in the magnetic alignment field induce relaxation in proportion to the diffusion constant for the cell and the square of the gradients transverse to the magnetic alignment field [23]. This effect was very small ($\tau_{\nabla B}$ >500 hours) in the high-density SLAC target, but in experiments where spectrometer magnets are close to the target, the field gradients can be much more important. Nuclear relaxation can also be induced by the presence of ionizing radiation such as an electron beam [24,25]. When a ^{3}He atom is ionized, the hyperfine interaction couples the nuclear spin to the unpaired electron spin allowing a transfer of angular momentum if the two initially have opposite spin orientations. Furthermore, electrons from other ^{3}He atoms can be transferred to the original ion, creating the potential for depolarizing another atom. This depolarization process continues until the ions are finally neutralized. Under the conditions in our target (high ^{3}He density and an admixture of nitrogen), the number of ^{3}He nuclear depolarizations per ^{3}He ion created is 0.62±0.08 according to [25]. Only at the highest currents used was there any effect on the ^{3}He polarization. The relaxation time inferred by this drop in ^{3}He polarization is greater than 190 hours at our maximum beam current of 3.5 μA, and the predicted time constant from [25] is 250 hours. The total ^{3}He nuclear relaxation rate is given by

$$\frac{1}{\tau_R} = \frac{1}{\tau_{cell}} + \frac{1}{\tau_{beam}} + \frac{1}{\tau_{\nabla B}} \tag{4}$$

when these two external mechanisms are included.

CELL PRODUCTION

The goal for cell development is to minimize the effect of the walls and gas impurities on the nuclear polarization. The first step in combating these problems is to construct the entire cell from aluminosilicate glass. It is postulated that the extremely small ^{3}He relaxation induced by this glass is due to its very low permeability for helium. Since a ^{3}He atom does not get trapped for long at the surface during a collision with the wall, interactions will be of short duration, reducing the probability of inducing nuclear spin flips. The ^{3}He cells used in [10] and [26] demonstrated that relaxation due to the aluminosilicate glass can be reduced to a negligible level compared to bulk relaxation.

For the SLAC target, we needed to consistently approach the limit of τ_{bulk} in a cell of more complex geometry and larger volume. For this purpose untreated commercial tubing is completely unsatisfactory. The first step in treating the tubing is to carefully reblow all the glass that forms the target cell by resizing the tubing. For instance, the target chamber glass tubing is initially 12 mm in diameter and is expanded to 21 mm on a glass working lathe. With this procedure the entire cell wall becomes molten so that when it re-forms, it leaves a pristine surface presumably with fewer contaminants and defects. Since aluminosilicate glasses are hard to work, before adopting the resizing method, we tried simply rinsing the glass with nitric acid to remove any surface contaminates. The acid cleaning did improve τ_{wall} dramatically, increasing it from as little as tens of minutes to a few hundred hours. Unfortunately, $\tau_{\rm cell}$ tended to decay significantly with time in the high-pressure, 5 to 10 atm cells. Low pressure (1 atm) cells do not exhibit this effect, as far as limited tests have shown.

Equally important to the construction methods is the filling process. The cells are attached to a high vacuum system ($\approx 10^{-7}$ to 10^{-8} Torr) and baked out under vacuum for 3 to 6 days at 475 °C (Fig.2). The Rb is then distilled into the cell with a hand held torch from a secondary chamber of the vacuum system. Next, a small amount of nitrogen (99.9995% pure) is frozen into the cell. Finally, the initially 99.995% chemically pure ^{3}He is introduced into the cell through a trap at liquid ^{4}He temperature. This cryogenic trap further purifies the ^{3}He by condensing out any contaminants. The cell is also cooled with liquid ^{4}He in order to get a high density of ^{3}He in the cell while maintaining a pressure of less than an atmosphere. This step is necessary since the cell is permanently sealed by melting closed a constriction in the glass tube where the cell attaches to the vacuum system. Similar cell filling procedures were used for experiments at TRIUMF [13,27] and at LAMPF [10,26].

When this combination of construction technique and filling procedure was followed, out of ten cells produced, all five of those measured had nuclear polarization lifetimes in excess of 30 hours. Three of the five cells, including all those used in the experiment, had measured lifetimes of 50 to 65 hours at room temperature. These numbers, compared to the 95 hour limit of τ_{bulk} at 20°C, imply that most of the relaxation is caused by the unavoidable ^{3}He–^{3}He dipole interaction, although some improvement in $\tau_{\rm cell}$ is still possible. Use of this procedure should ensure production of nearly bulk-limited lifetimes in target cells of any arbitrary geometry and volume so long as extreme care is taken to ensure the cell surfaces are all freshly worked glass, the bakeout is meticulous, the vacuum is good, and filling gases are well cleaned.

The net cell relaxation time is estimated to be about 70 hours when the cell is hot. From (4) and (1), we then find that the ^{3}He polarization is approximately 57% to 64% of $\langle P_{\rm Rb}\rangle$, for maximum and minimum electron beam current, respectively. One of the most important limitations is a small γ_{SE} caused by the low Rb number densities at our operating temperature of 160 to 165°C. There was sufficient laser power to run at even higher [Rb], but problems with oven materials overheating limited the temperature. Redesigning the oven with high temperature plastics should therefore allow higher [Rb], and a faster γ_{SE}. With this simple improvement, a doubling of the spin-exchange rate may be possible, leading to a factor of 1.25 improvement in $P_{^3\rm He}$.

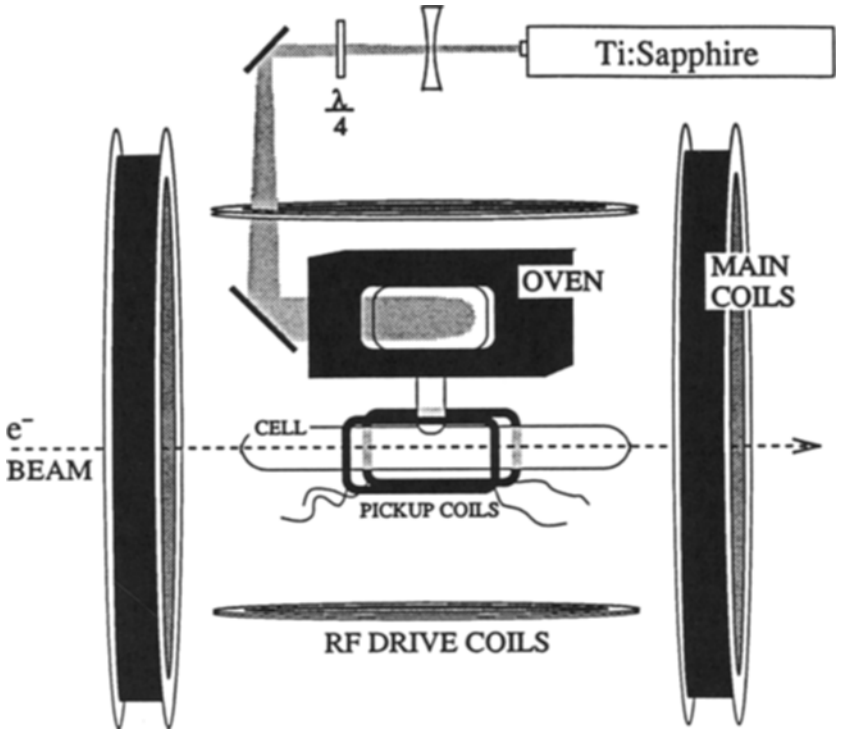

Fig. 1 Diagram of target system.

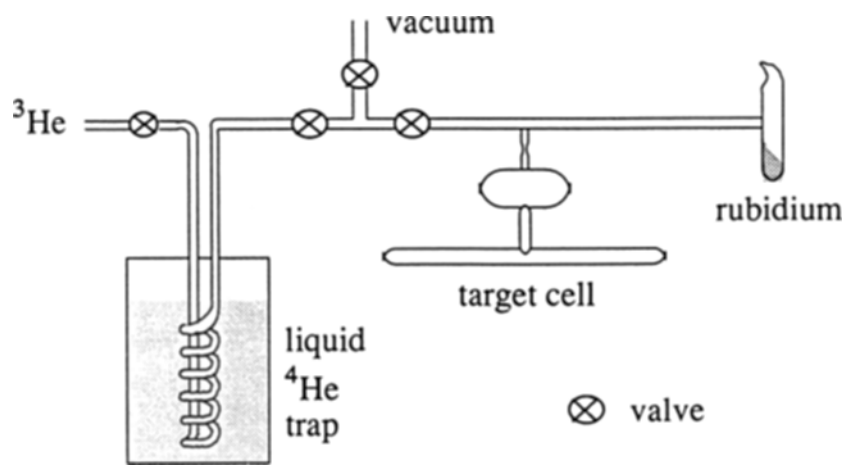

Fig. 2 Schematic of vacuum system.

I. NMR POLARIMETRY

The polarization measurements were made with the Nuclear Magnetic Resonance technique of Adiabatic Fast Passage (AFP) [20]. The AFP system uses a set of 18 inch Helmholtz drive coils to provide a 92 kHz RF field while the main alignment field is swept through the 29 G ^{3}He resonance. At resonance all the ^{3}He nuclear spins flip over inducing a signal in an orthogonal set of smaller pick-up coils located around the center of the target chamber of the cell. One possible concern is that the local polarization in the beam may be different from the target chamber's volume-average polarization measured by this system. However, with diffusion times on the order of seconds compared to tens of hours for relaxation and spin-exchange times, it is not possible to maintain any significant polarization gradient in the cell.

The AFP-NMR signal is calibrated with the known thermal equilibrium Boltzmann polarization of the protons in a water sample of the same dimensions. The value of the polarization is easily calculable from Boltzmann statistics and is given by

$$P_{proton} = \tanh\left(\frac{h\nu}{2k_BT}\right) \tag{5}$$

where B=22 G for protons in resonance with the 92 kHz RF. Typical proton signals are $\approx$ 1.8μV, and the resulting calibration for ^{3}He signals is 1.61 $\pm$ .11 % polarization per 10 mV of signal. Figure 3 shows a ^{3}He signal and an average of 25 proton signals.

We are also in the process of developing an alternate polarimetry method which involves measuring the shift in frequency of the Rb ESR line due to the magnetic field produced by the polarized ^{3}He [10,22]. This technique depends on an atomic calibration constant which at present is known to $\approx$ 3%.

II. TARGET PERFORMANCE

During the experimental run, the ^{3}He polarization was measured every four hours. The results of these measurements, which were taken from November 7 to December 22, 1992, are shown in Fig. 4. The average ^{3}He polarization over the entire run is about 36%. During the first three weeks of the experiment, there were a few precipitous drops in the polarization. These problems were caused by materials overheating in the pumping chamber oven, leading to mechanical failure of vacuum seals. The use of high temperature plastics in constructing the oven would easily correct this deficiency. Once further oven problems were avoided by operating at a lower temperature, the target polarization became very stable, running for three weeks with only slow drifts. Toward the end, the drop off in polarization due to an increased beam current is noticeable.

Overall the target required very little maintenance. The laser systems ran for days before requiring brief tuning, collectively producing 16 to 22 Watts. Target helicity reversals were easily done by rotating the alignment field and reversing the laser helicity, requiring only 10 minutes to complete. No other system required any significant attention during the latter half of the run.

Overall, the SLAC target was highly successful, and considering the conservative approach taken in designing this target, there is room for improvement. The target operated at a ^{3}He density of 2.3 $\times$ 10^{20} atoms/cm^3 in a 30 cm long scattering region. The target thickness of 7 $\times$ 10^{21} atoms/cm^2 is the highest yet achieved in a polarized ^{3}He target. This high density provides good statistics in spite of a moderately large background event rate, which accounted for about two thirds of the events. Ten to twenty percent increases in ^{3}He density along with at least a factor of two reduction in background rates from using thinner windows should be realized in future target cells. The long ^{3}He spin-relaxation times of the target cells, estimated to be 70 hours at 65°C, led to an average polarization of 36% and a maximum of 42%. The possibility exists for small improvements in target cell lifetimes and a factor of two

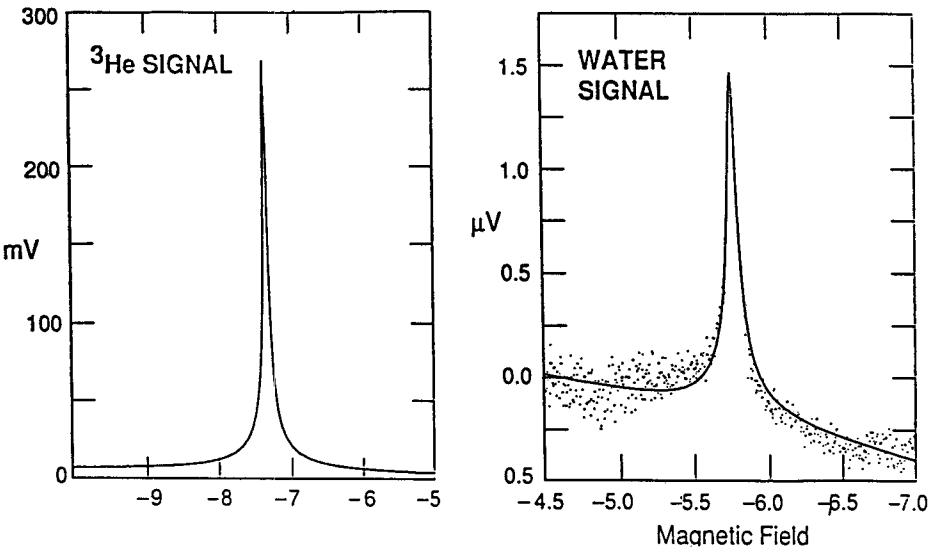

Fig. 3 NMR signals from He cell and water sample.

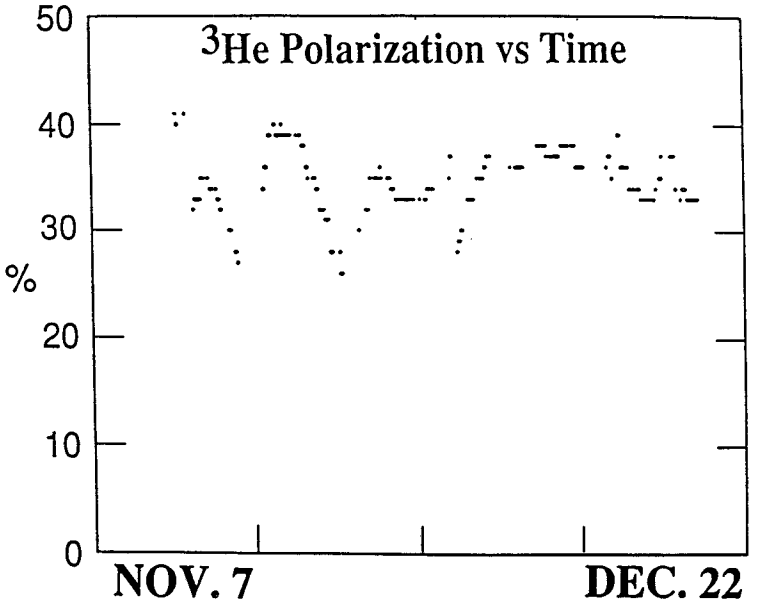

Fig. 4 Evolution of the target polarization during the six week experimental run.

in spin-exchange time. This combination could bring the ^{3}He polarizations well into the 50% range. Even without these improvements, the performance of this ^{3}He target was excellent and was central to conducting the most sensitive nuclear spin-dependent structure function measurement to date.

---

[1] F.D. Colegrove, L.D. Schearer and G.K. Walters, Phys. Rev. **132**, 2561 (1963).

[2] B. Blankleilder and R.M. Woloshyn, Phys. Rev. **C29**, 538, (1984); R.M. Woloshyn, Nucl. Phys. **496A**,749 (1989).

[3] R.G. Milner, Proc. Workshop on Polarized ^{3}He beams and Targets, ed. R.W. Dunford and F.P. Calaprice, AIP Conf. Proc. **131**, (AIP, New York 1985), p. 186.

[4] P.L. Anthony *et al.*, accepted for publication, Phys. Rev. Lett. **71**, 1993.

[5] V.W. Hughes and J. Kuti, Ann. Rev. Nuc. Sci. **33**, 611 (1983).

[6] B. Adeva *et al.*, Phys. Lett. B **302**, 533 (1993).

[7] M.A. Bouchiat, T.R. Carver and C.M. Varnum, Phys. Rev. Lett. **5**, 373 (1960).

[8] N.D. Bhaskar, W. Happer, and T. McClelland, Phys. Rev. Lett. **49**, 25 (1982).

[9] W. Happer, E. Miron, S. Schaefer, D. Schreiber, W.A. van Wijngaarden, and X. Zeng, Phys. Rev. A **29**, 3092 (1984); X. Zeng, Z. Wu, T. Call, E. Miron, D. Schreiber, and W. Happer, Phys. Rev. A **31**, 260 (1985).

[10] N.R. Newbury *et al.*, Phys. Rev. Lett. **67**, 3219 (1991);N.R. Newbury *et al.*, Phys. Rev. Lett. **69**, 391 (1992).

[11] T.E. Chupp, M.E. Wagshul, K.P. Coulter, A.B. McDonald, and W. Happer, Phys. Rev. C **36**, 2244 (1987).

[12] T.E. Chupp, R.A. Loveman, A.K. Thompson, A.M. Bernstein, and D.R. Tieger, Phys. Rev. C **45** 915 (1992).

[13] B. Larson *et al.* Phys. Rev. Lett. **67**, 3356 (1991).

[14] W. Heil, this proceedings.

[15] M. Leduc *et al.*, Nucl. Sci. Appl. 1, 1 (1983); C.L. Bohler *et al.*, J. Appl. Phys. **63**, 2497 (1988).

[16] R.G. Milner, R.D. McKeown, and C.E. Woodward, Nuc. Inst. Meth. in Phys. Res. **A 274**, 56 (1989); K. Lee *et al.*, Phys. Rev. Lett. **70**, 738 (1993).

[17] L.D. Schearer, private communication.

[18] N.D. Bhaskar, M. Hou, B. Souleman, and W. Happer, Phys. Rev. Lett. **43**, 519 (1979);R.J. Knize, Phys. Rev. A **40**, 6219 (1989).

[19] R.L. Gamblin and T.R. Carver, Phys. Rev. **138**, A946 (1965).

[20] A. Abragam, Principles of Nuclear Magnetism (Oxford University Press, New York, 1961).

[21] W. Hersman, these proceedings.

[22] N.R. Newbury, A.S. Barton, P. Bogorad, G.D. Cates, M. Gatzke, H. Mabuchi, and B. Saam, Phys. Rev. A **48**, 558 (1993); A.S. Barton, N.R. Newbury, G.D. Cates, B. Driehuys, H. Middleton, B. Saam, submitted to Phys. Rev. A, (May 1993).

[23] G.D. Cates, S.R. Schaefer and W. Happer, Phys. Rev. A **37**, 2877 (1988); G.D. Cates, D.J. White, Ting-Ray Chien, S.R. Schaefer and W. Happer, Phys. Rev. A **38**, 5092 (1988).

[24] K.D. Bonin, T.G. Walker, and W. Happer, Phys. Rev. A **37**, 3270 (1988).

[25] K.P. Coulter, A.B. McDonald, G.D. Cates, W. Happer, T.E. Chupp, Nuc. Inst. Meth. in Phys. Res. **A276**, 29 (1989).

[26] N.R. Newbury, A.S. Barton, G.D. Cates, W. Happer, and H. Middleton, submitted to Phys. Rev. A (December, 1992).

[27] B. Larson, O. Häusser, P.P.J. Delheij, D.M. Whittal, and D. Thiessen, Phys. Rev. A **44**, 3108 (1991).